Pergamon

Tetrahedron: Asymmetry, Vol. 7, No. 9, pp. 2655-2664, 1996

0957-4166/96 $15.00 + 0.00

PII: S0957-4166(96)00341-2

$HB(OH)_2$ and H_2CO as Probes for a Study on Binding of Dialkoxyboranes and Ketones to Oxazaborolidines Capable of Catalyzing the Enantioselective Reduction of Ketones

Vesa Nevalainen

Laboratory of Organic Chemistry, P.O. Box 55, SF-00014 University of Helsinki, Finland

Abstract: - Dihydroxyborane - formaldehyde adducts of oxazaborolidine were used as models of alkoxyborane - ketone adducts of chiral oxazaborolidines (*e.g.* **1**) being potentially involved as intermediates in the enantioselective reductions (catalyzed by **1**). The models were studied by means of *ab initio* MO methods. Energies (MP2/6-31G*//MP2/6-31G*) of the formation of $HB(OH)_2$ - H_2CO adducts were clearly negative (e.g. - 94 kJ mol^{-1}) but only about 70% of that of the corresponding H_2BOH adduct. In all these adducts both ends of H_2CO were bound (H_2CO as a bidentate ligand). Isomeric monodentate adducts were predicted to be unstable. Optimization (MP2/6-31G*) of one conformer of the monodentate adducts led to the corresponding bidentate adducts whereas in the case of another conformer a hydride transfer [from the $HB(OH)_2$ moiety to the H_2C=O one] followed by opening of the oxazaborolidine ring took place (ΔE = -246 kJ mol^{-1}).

INTRODUCTION

Chiral oxazaborolidines (e.g. **1**) have been shown to function as efficient catalysts for the enantioselective reduction of ketones.[1] In the case of borane as a source of hydrogen formation of the dialkoxyborane derivative of the newly formed chiral alcohol has been observed[1b] (only two of three of the hydrogens of H_3B utilized). Ketone - alkoxyborane adducts (e.g. **2**; the ketone as a bidentate ligand) of oxazaborolidines have been predicted to be stable.[2] Also **3**, being closely analogous to **2**, could exist, and be formed, for example, *via* **4**. As the reduction catalyzed by **1** stops at the dialkoxyborane level either the formation of **4** (unstable ?) or the third hydride transfer (formation of trialkoxyboranes) must be disfavored.

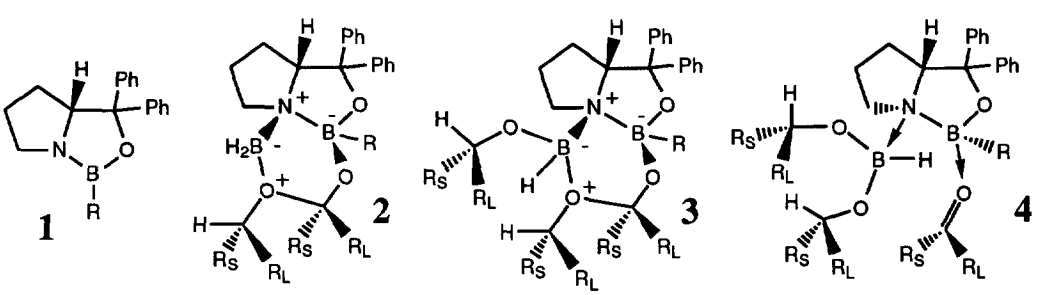

It is not yet fully understood why only two of the total of three hydrogens of the reacting borane (H_3B) can be utilized in the reduction. One way to learn more about the factors determining the outcome of these

reductions could be to inspect plausible interactions of starting materials and products with the catalyst. Such interactions could be related to mechanisms of (in)activation of the catalysts. As recent computational studies on small models (e.g. **2a**) indicate the formation of **2** to be thermodynamically advantageous, the aim of this work was chosen to probe the related dialkoxyborane analogs **3** and one (i.e. **4**) of plausible precursors of **3**.

MODELS AND METHODS

The simple analogs **1a**, **2a**, **3a-b** (*endo*-OH), **3c** (*exo*-OH) and **4a-b** were used as models of **1** - **4**. All these models were studied using *ab initio* MO methods. Gaussian 94[3] was employed in all calculations. All models were optimized at the MP2/6-31G* level.

The starting geometry of **4a** [the *O*-lone pairs of $HB(OH)_2$ *syn*; the non-coordinated OH in an *endo* conformation] was provided by substituting one of the hydrogens of the corresponding hydroxyborane adduct (studied earlier)[2] by an OH group and reoptimizing the resulting model at the 3-21G level.[4] The model **4b** [lone pairs of $HB(OH)_2$ *syn*] was generated[4] by rotating the B-O bond of the *endo*-OH group of **4a** (3-21G//3-21G).[4]

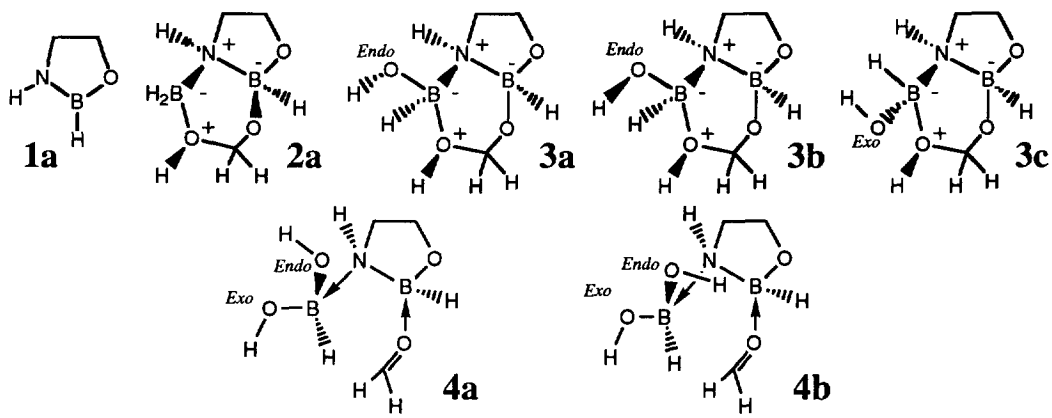

RESULTS AND DISCUSSION

A stereoscopic view of the optimized structure of **3a** (compared with that of **2a**) is shown in Figure 1 whereas the optimized structures of conformers **3b-c** (compared with that of **3a**) are shown in Figure 2. Both of the models **4a**[4] and **4b**[4] were found unstable (at the MP2/6-31G* level). Model **4a**, while being optimized, was transformed to **3a** (Fig. 3; pathway **4a** -> **A** -> **B** -> **C** -> **3a**) whereas in the model **4b** a hydride transfer [from the $HB(OH)_2$ moiety to the $H_2C{=}O$ one] took place (Fig. 3; pathway **4b** -> **D** -> **E** -> **F** -> **G**). Energies, dipole moments, selected charges and selected sp^n ($2 \leq n \leq 3$) hybridizations of the optimized models (except those of **4a** and **4b** found unstable) are shown in the Table.

As these calculations (particularly those related to the models **4a** and **4b**; Fig. 3) were very time consuming, optimization of neither one of the intermediates **C** or **G** (Fig. 3) was continued to the corresponding stationary point. This was considered as a rational approach because an independent optimization of **3a** had already been carried out (Fig. 1) and because the results (also in the case of the intermediate **G**) allow very clear conclusions to be drawn, respectively.

Table. Energies, dipole moments, partial charges and sp^n hybridizations (MP2/6-31G*//MP2/6-31G*).[a-f]

Struct. #	E[a]	D[b]	E_R[c]	$Q_{bor.}$[d]	Q_{H2CO}[e]	n of sp^n (hybridizations)[f]				
						(C_{CO})	($B_{cat.}$)	(B_{BO2})	($N_{cat.}$)	($O_{BO2\text{-}6\text{-}ring}$)
1a	-233.96765	2.74	-	-	-	-	2.00	-	2.00	-
2a	-449.76389	3.88	-134	-0.001	-0.033	2.61	2.69	3.00	2.89	3.00
3a	-524.85841	4.64	-94	+0.022	-0.040	2.65	2.67	3.00	2.92	3.00
3b	-524.84970	3.78	-71	+0.052	-0.038	2.66	2.66	3.00	2.89	2.85
3c	-524.85569	5.27	-87	+0.033	-0.041	2.62	2.68	2.99	2.94	3.00
H_2B-OH	-101.57769	1.71	-	-	-	-	-	2.0	-	-
$HB(OH)_2$	-176.68715	1.75	-	-	-	-	-	2.0	-	-
H_2C=O	-114.16775	2.84	-	-	-	2.00	-	-	-	-

[a] Total energies (E) given in hartrees. [b] Dipole moments (D) given in debyes. [c] Energies (E_R) relative to **1a** + (di)hydroxyborane + H_2CO given in kJ mol^{-1}. [d] The charge (Q_{bor}) of the (di)hydroxyborane moiety. [e] The charge (Q_{H2CO}) of the formaldehyde moiety. [f] Atoms which the n-values ($2 \le n \le 3$; ref. 2) are related to are shown in parentheses.

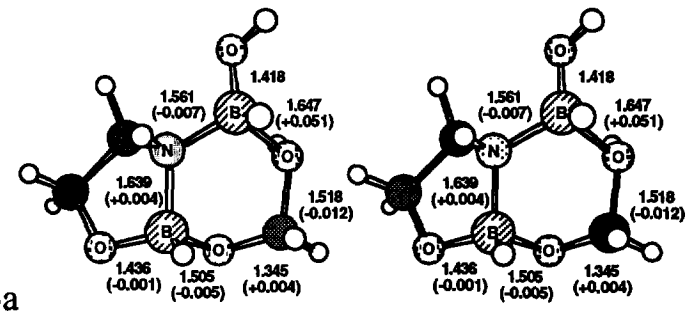

3a

Bond angles	2a	3a[a]
B_{BO2}-N-B	118.0°	+1.3°
N-B-O_{CO}	104.7°	-0.3°
B-O_{CO}-C_{CO}	112.4°	0.0°
O_{CO}-C_{CO}-O_{BO2}	109.7°	+0.5°
C_{CO}-O_{BO2}-B_{BO2}	113.0°	+1.6°
O_{BO2}-B_{BO2}-N	106.8°	-1.8°
N-B_{BO2}-O_{OH}	112.6°[b]	-2.6°
N-B-$O_{catal.}$	102.7°	-0.5°
O_{BO2}-B_{BO2}-O_{OH}	105.0°	0.0°

[a] Relative to **2a**. [b] The value of the corresponding N-B-H angle

Torsion angles	2a	3a[a]
B_{BO2}-N-B-H	+73.7°	-2.2°
B_{BO2}-N-B-O_{CO}	-46.0°	-2.7°
B_{BO2}-O-C_{CO}-O_{CO}	+63.0°	-3.0°
C_{CO}-O_{CO}-B-O	+173.0°	+0.8°
N-B_{BO2}-O_{BO2}-H	+74.7°	+3.1
O_{BO2}-B_{BO2}-O_{OH}-H	-	-88.6[b]

[a] Relative to **2a**. [b] The absolute value

Figure 1. A stereoscopic view of the optimized (MP2/6-31G*//MP2/6-31G*) structure of **3a**. Selected bond lengths [in Å] are shown. Changes of bond lengths related to the hypothetical substitution of one of the hydrogens of H_2BOH by a hydroxyl group (i.e. **2a** -> **3a**) are shown in parentheses [negative (positive) values imply shortening (lengthening) of the bond].

Structural characterization of the chelates 3a-c

Overall structural parameters of the adducts **2a** and **3a-c** (i.e. bond lengths, bond angles and torsion angles) are closely similar (Figures 1 and 2). The most significant difference can be seen in the binding of the

oxygen (O_{bridge}) connecting the H_2C=O and $HB(OH)_2$ moieties. The B_{BO2}-O_{bridge} bonds of **3a-c** (1.651 ± 0.006 Å) are 0.055 Å longer than the corresponding bond of **2a** (Figures 1 and 2). The adjacent C_{CO}-O_{bridge} bonds of **3a-c** (1.516 ± 0.006) appear to be only 0.015 Å shorter than the corresponding bond of **2a**. All the other differences related to bond lengths of **2a** and **3a-c** are smaller than 0.015 Å, respectively.

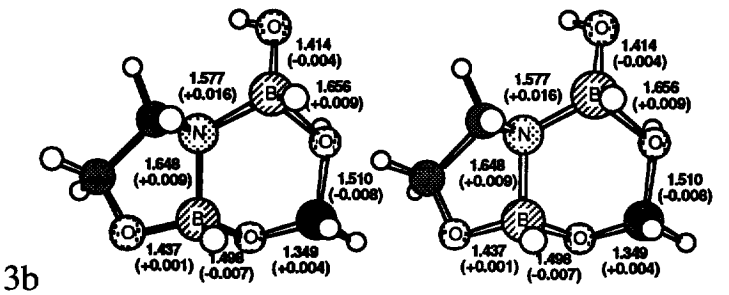

3b

Bond angles	3b[a]	3c[a]
B_{BO2}-N-B	-0.7°	+0.4°
N-B-O_{CO}	-0.1°	+0.6°
B-O_{CO}-C_{CO}	-0.2°	-0.6°
O_{CO}-C_{CO}-O_{BO2}	+0.2°	-0.8°
C_{CO}-O_{BO2}-B_{BO2}	+1.3°	-1.6°
O_{BO2}-B_{BO2}-N	0.0°	+0.3°
N-B_{BO2}-O_{OH}	+5.9°	-2.5°
N-B-$O_{catal.}$	-0.2°	+0.1°
O_{BO2}-B_{BO2}-O_{OH}	+0.4°	+2.3°

[a] Relative to **3a**

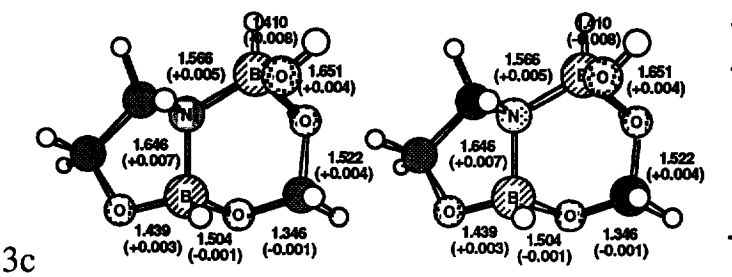

3c

Torsion angles	3b[a]	3c[a]
B_{BO2}-N-B-H	-0.6°	+3.5°
B_{BO2}-N-B-O_{CO}	-1.0°	+3.5°
B_{BO2}-O-C_{CO}-O_{CO}	-2.2°	+3.9°
C_{CO}-O_{CO}-B-O	+1.7°	-0.9°
N-B_{BO2}-O_{BO2}-H	+6.2°	-2.4°
O_{BO2}-B_{BO2}-O_{OH}-H	+179.9°	+171.6°

[a] Relative to **3a**

Figure 2. A stereoscopic view of the optimized (MP2/6-31G*//MP2/6-31G*) structures of **3b** and **3c**. Selected bond lengths [in Å] are shown. Bond lengths relative to those of **3a** are shown in parentheses [negative (positive) values imply shortening (lengthening) of the bond].

A comparison of structural parameters of **3a** [*endo* -OH; *anti* lone pairs of $HB(OH)_2$] and **3c** [*exo* -OH; *anti* lone pairs of $HB(OH)_2$] with those of **3b** [*endo* -OH; *syn* lone pairs of $HB(OH)_2$] reveals that structural changes related to the orientation of the *O*-lone pairs (structural differences between **3a** and **3b**; Figures 1 and 2) are larger than those related to the orientation (*endo/exo*) of the hydroxyl group itself (structural differences between **3a** and **3c**; Figures 1 and 2). Relative energies of the adducts (E_R; the Table) imply the same: **3a** is only 7 kJ mol^{-1} more stable than **3c** ($\Delta E_{endo/exo}$) whereas the corresponding difference between **3a** and **3b** is three times larger [i.e. 23 kJ mol^{-1} ($\Delta E_{syn/anti}$)]. Because the orientation of lone pairs of O_{BO2} appears to affect the electron structure and stability of these adducts an inspection of electrostatics of the adducts could be revealing.

Dipole moments (the Table) of the adducts **3a** and **3c** [*anti* lone pairs of $HB(OH)_2$] are higher than the moment of **3b** (*syn* lone pairs). The same relation between **3a** (or **3c**) and **3b** can be seen also as the partial charges of the $HB(OH)_2$ moieties ($Q_{bor.}$) of **3a-c** are compared (the Table). The partial charge of **3b** ($Q_{bor.}$=+0.052, the Table) is considerably higher than that of **3a** (+0.022) or **3c** (+0.033). Interestingly, the charge of the H_2CO moiety (Q_{H2CO}) remains almost as a constant in **3a-c** (as do the sp^n hybridizations; the Table). This implies that introduction of a factor of instability (e.g. by increasing ring strain) in the 6-ring system of this type of chelates would affect the N-B_{BO2} interaction (more flexible) before the B-O_{CO} one (less flexible). The same conclusion can be drawn if the partial charges ($Q_{bor.}$) of the hydroxyborane moieties of **2a** and **3a-c**

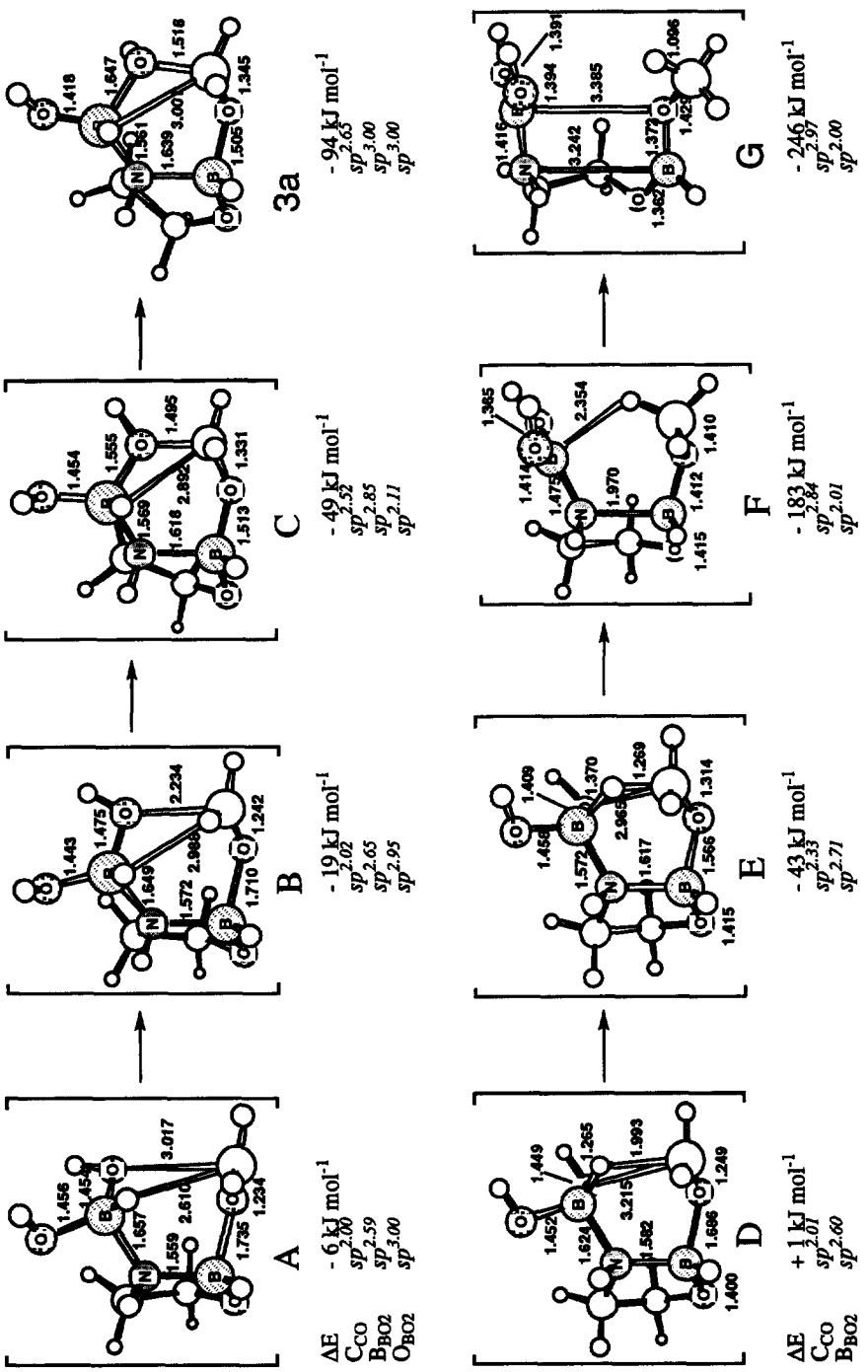

Figure 3. Some intermediates (**A** - **G**) observed when **4a** and **4b** were optimized (MP2/6-31G*). None of the intermediates represents a stationary point. Selected bond lengths (in Å), energies [relative to **1a** plus $HB(OH)_2$ plus $H_2C{=}O$] and sp^n-hybridizations are shown below the structures.

are compared (Fig. 4) with the corresponding energies (E_R, the Table). The higher is the positive charge on the (di)hydroxyborane moiety the less stable would be the chelate (Fig. 4). Changes of the charge (Q_{H2CO}) of the H_2CO moiety are much less significant [as compared with the changes of $Q_{bor.}$, Fig. 4].

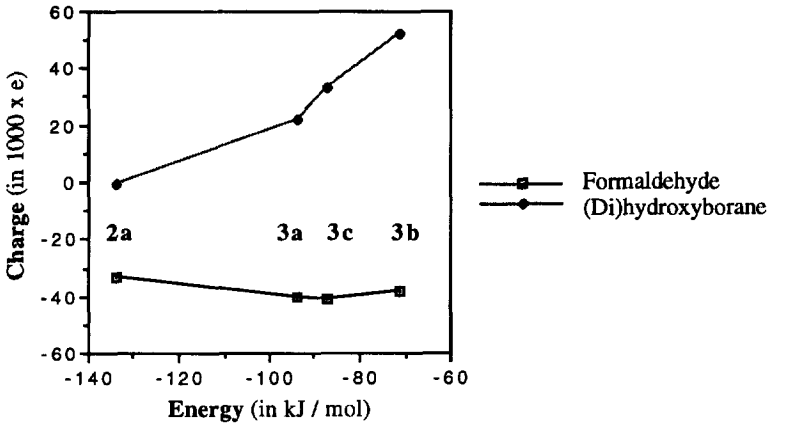

Figure 4. Correlation of the charges ($Q_{bor.}$ and Q_{H2CO}, the Table) of formaldehyde and (di)hydroxyborane moieties with the stability (E_R, the Table) of the chelates **2a** and **3a-c**.

*Characterization of the monodentate adducts **4a*** and ***4b***

The adducts **4a** and **4b**[4] were found to be unstable. All attempts to optimize the rough[4] models **4a** and **4b** at the MP2/6-31G* level were "unsuccessful". Results of those optimizations are summarized in Figure 3.

During the optimization of the model **4a** the B-O_{CO} and N-B_{BO2} bonds got rotating (**A** -> **B**; Fig. 3) so that the H_{BO2} - C_{CO} distance, although shortened, remained shorter than the O_{BO2} - C_{CO} one (i.e. the O_{BO2} - C_{CO} "gap" remained broader than the H_{BO2} - C_{CO} one). Also the sp^n hybridizations of C_{CO}, B_{BO2} and O_{BO2} remained unaffected (Fig. 3). After that binding interactions between $HB(OH)_2$, H_2CO and the oxazaborolidine tightened substantially (formation of **C**, Fig. 3). In **C** the oxygen of $HB(OH)_2$ being coordinated to C_{CO} is still almost sp^2 hybridized [n of $sp^n(O_{BO2})$ is 2.11 in **C**; Fig. 3]. Hybridizations of the other atoms got already almost to the level of **3a** (Fig. 3). The B-O bonds of the $HB(OH)_2$ moiety were, however, still considerably different from those of **3a**. Therefore, it looks as if the carbonyl - oxazaborolidine moiety would, firstly get organized [by changes related to torsion angles (small energy changes)] in a geometry in which simple changes of bond lengths would lead to the chelation (formation of the "hot" chelate **C**; Fig. 3) and release of about one half of the total energy of formation of **3a**.

"Cooling" [lengthening/shortening of the B-O bonds of $BH(OH)_2$ and rehybridization of the chelating oxygen; other structural changes are clearly less significant; Fig. 3] of the hot chelate **C** would release the other half of the energy (of formation of **3a**). On the basis of these observations it looks as if the bidentate chelation (formation of **3**) could be favoured over the hydride transfer if one of the lone pairs (*cis* to the adjacent hydride) of the oxygen of the alkoxyborane moiety of **4** would be oriented towards the carbonyl (as in the case of **4a**). In order to assess steric crowd potentially related to the formation of chelates analogous to **3** an extended model (corresponds to the case in which acetophenone would be the ketone being reduced) of the intermediate **C** (Fig. 3) was constructed as shown in Figure 5 (standard bond lengths and angles were used for the groups added).

On the basis of the rough model (Fig. 5) of **C** one could draw a conclusion that the 1-phenylethyl substituent of the chelating oxygen could hardly turn (needed for the the sp^2 -> sp^3 change of the chelating oxygen; analogous to **C** -> **3a**, Fig. 3) significantly closer to one of the 5,5-diphenyl groups (Fig. 5). Therefore, in the case of most enantioselective reductions catalyzed by oxazaborolidines (e.g. **1**) the bidentate chelates (if formed) could structurally resemble more the intermediate **C** than **3a** (Fig. 5). Another reaction would be favoured if the lone pairs of the *endo*-OH are turned away from the carbonyl (as in **4b**).

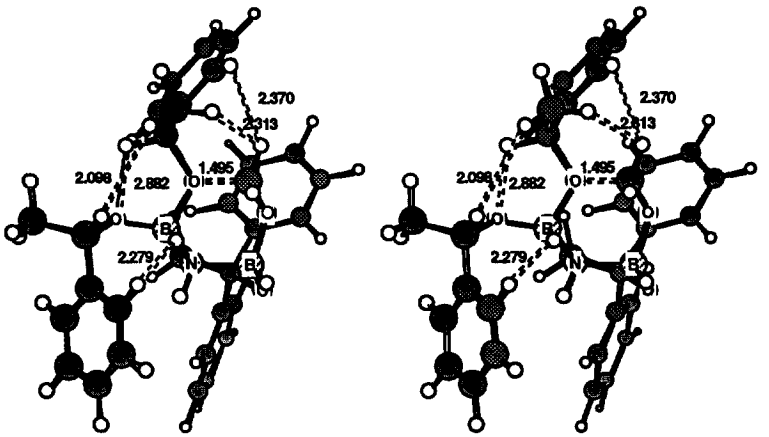

Figure 5. Stereoscopic presentation of an extended model (not optimized) of the intermediate C (Fig. 3). The model was generated by substituting hydrogens of both OH groups of $HB(OH)_2$ of C (Fig. 3) by (*S*)-1-phenylethyl groups (corresponds to the reduction of acetophenone). Some non-bonded interactions [except that (1.495 Å) between O_{BO2} and C_{CO}] are shown (values in Ångströms).

During the optimization of **4b** the B-O_{CO} and N-B_{BO2} bonds got rotating (**4b** -> **D**; Fig. 3) so that the H_{BO2} - C_{CO} distance shortened while the O_{BO2} - C_{CO} one lengthened (i.e. the O_{BO2} - C_{CO} "gap" broadened while the H_{BO2} - C_{CO} one narrowed). These structural changes did not release energy (ΔE = +1 kJ mol^{-1}) or involve hybridizational changes in the H_2CO / $HB(OH)_2$ moieties (Fig. 3). The intermediate **D** (Fig. 3) is interesting in that the H-O_{BO2} bonds point almost to the same direction. This orientation, however, would require (e.g. in the case of enantioselective reduction of acetophenone catalyzed by **1**) the alkyl groups of the newly formed chiral alcohol to be placed so that the groups would have (a number of) non-bonded (highly) repulsive interactions. In order to illustrate the level of steric crowd attributable to the presence of the alkyl groups an extended model of **D** was constructed (Fig. 6). The model (Fig. 6) was created by substituting hydrogens of the $HB(OH)_2$ moiety of **D** (Fig. 3) with (S)-1-phenylethyl groups and both of the hydrogens of *C5* (of the oxazaborolidine ring) by phenyl groups (standard bond lengths and angles were used).

The model shown in Figure 6 indicates that there would be steric crowd related not only to interactions between the two (*endo* and *exo*) 1-phenylethyl groups [of which the 1-hydrogens hardly could reside at a distance of 1.522 Å ! as they do in the extended model; Fig. 6] but also to interactions between one of the 5-phenyls (of the oxazaborolidine ring) and the inner (*endo-O*) phenylethyl group (short distances between 2.033 - 2.195 Å; Fig. 6). On the basis of the above inspection of the extended model (Fig. 6) one could conclude that in the enantioselective reduction of ketones catalyzed by oxazaborolidines the reduction may stop at the dialkoxyborane level because the reactive intermediate (analogous to that shown in Fig. 6) potentially important for the hydride transfer would be sterically too crowded and therefore would not be formed.

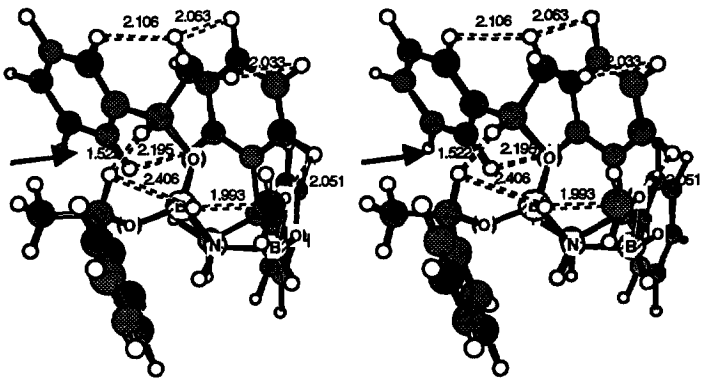

Figure 6. A stereoscopic presentation of an extended model (not optimized) of the intermediate **D** (Fig. 3). The model was generated by substituting both hydrogens of the OH groups of $HB(OH)_2$ of **D** (Fig. 3) by (*S*)-1-phenylethyl groups (corresponds to the reduction of acetophenone). Some non-bonded (potentially highly repulsive, see the arrow) interactions [except that (1.993 Å) between H_{BO2} and C_{CO}] are shown (values in Ångströms).

Structural changes related to the formation of the unstable hydride-bridged system (**D** -> **E**; Fig. 3) affect the bond lengths of **D** (more than the related bond angles). Although the hydride resides in between (or almost in the middle of) the C_{CO} and B_{BO2} atoms of the "hot" intermediate **E** (Fig. 3) it has significantly affected hybridization of neither the hydride acceptor [Δn of sp^n (C_{CO}) is +0.32, i.e. only ≈ 30% of that of the complete reaction **4b** -> **G**; Fig. 3] nor the donor [Δn of sp^n (B_{BO2}) is +0.11, i.e. only ≈ 20% of that of the complete reaction **4b** -> **G**; Fig. 3]. These observations imply the hydride transfer to occur in a very early phase of the reaction pathway. The hydride transfer itself does not release energy (ΔE of **E** is -43 kJ mol^{-1}) more than the related chelation in the case of **4a** (i.e. **4a** -> **C**; Fig. 3). The highly negative ΔE related to the reaction **E** -> **F** (Fig. 3) suggests that rehybridization taking place in the hydride-bridged 6-ring of **E** (Fig. 3) and related changes of bond lengths and angles could be (one of) the major sources of energy released in these reductions.

In the case of the hydride transfer (Fig. 3) it is difficult to detect when the reduction is complete. The hydride transfer step appears to be coupled with a cleavage of the oxazaborolidine ring (formation of **G**, Fig. 3). Furthermore, the cleavage starts before the hydride transfer is over. While the hybridization of C_{CO} in **F** is only at the level of $sp^{2.84}$ (indicating the reduction of the carbonyl moiety to be about 84% of that of the complete reaction) the B-N bond of the oxazaborolidine ring has lengthened substantially. The amount of energy liberated by the cleavage [ΔE(**F**,**G**) = 43 kJ mol^{-1}; Fig. 3] is near that of the formation of the hot intermediate **E** [ΔE = -43 kJ mol^{-1}; Fig. 3]. In the intermediate **G** (Fig. 3) the hybridizational changes related to the hydride transfer are, finally, practically complete [e.g. hybridization of C_{CO} is $sp^{2.97}$, i.e. ≈ 97% of that of the ideal reaction; also the hydride donor (B_{BO2}) is completely sp^2 hybridized in **G**]. No minimum (i.e. stationary point) was found in the pathway **4b** -> **D** -> **E** -> **F** -> **G** (Fig. 3) which indicates the hydride transfer to lead to the opening of the oxazaborolidine ring, as has been predicted earlier[5] in the case of borane (H_3B)[5] adducts analogous to **4**.

CONCLUSIONS

On the basis of the above inspection of $HB(OH)_2$ and H_2CO adducts of 1,3,2-oxazaborolidine it could be predicted, that monodentate coordination of ketones to dialkoxyborane (a derivative an enantiopure secondary

alcohol) adducts of 5,5-diphenyl-1,3,2-oxazaborolidines leads to (unstable) complexes which tend to react further *via* two pathways.

One of the pathways involves a hydride transfer (pathway **A**) from the dialkoxyborane moiety to the adjacent activated carbonyl system. The other pathway (pathway **B**) leads to the formation of a complex in which both atoms of C=O are bound to the dialkoxyborane - oxazaborolidine moiety (the carbonyl compound as a bidentate ligand). Which one of the pathways (**A** or **B**) is followed depends on the the orientation of the lone electron pair of the oxygen [of the sterically more hindered alkoxy group (*i.e.* the one residing closer to the oxazaborolidine ring) of the dialkoxyborane moiety] and its adjacent alkyl group.

Before the hydride transfer (pathway **A**) takes place, both the alkyl groups of the dialkoxyborane moiety are required to be oriented away (*i.e.* large C_{alkyl}-O-B_{BO2}-$N_{catal.}$ torsion angles) from the catalyst. In the case of dialkoxyboranes originating from the enantioselective reduction of ketones (catalyzed by 5,5-diphenyl-1,3,2-oxazaborolidines) this can hardly take place because of steric hindrance (the alkyl groups would be required to come too close together). Therefore, steric hindrance in the *N*-coordinated dialkoxyborane moiety could be considered as a major factor preventing [in the absence of the steric hindrance (e.g. in the case of dihydroxyboranes) a highly exothermic and spontaneous hydride transfer (accompanied with a cleavage of the B-N bond of the oxazaborolidine moiety) takes place] the utilization of the third hydride of borane (H_3B) used as a source of hydrogen in most oxazaborolidine catalyzed reductions.

The pathway **B** leading to the formation of bidentate adducts does not involve steric crowd similar to that of **A** although also formation of the bidentate adducts is energetically advantageous. Stability of the adducts depends on the orientation of the lone pairs of oxygen of the non-coordinated alkoxy group (of the dialkoxyborane moiety) more than the orientation of the alkoxy group itself. Formation of these bidentate adducts could prevent (both coordination sites of the catalyst are occupied) the oxazaborolidine involved from acting as a chiral catalyst for the enantioselective reduction of ketones. Further studies on properties of oxazaborolidines capable of acting as chiral catalysts are in progress.

ACKNOWLEDGEMENTS

The Physics Computation Unit (DEC 3000 M400 Alpha, Univ. of Helsinki), the Centre of Scientific Computing (Cray X-MP) and the Computing Centre (VAX 6000-610, Univ. of Helsinki) are acknowledged for providing computational resources needed for this study.

REFERENCES AND NOTES

1. (a) Masui, M.; Shioiri, T. *SYNLETT* **1996**, 49; (b) Corey, E. J.; Helal, C. J. *Tetrahedron Lett.* **1995**, *36*, 9153; (c) Sudo, A.; Matsumoto, M.; Hashimoto, Y.; Saigo, K. *Tetrahedron Asymmetry* **1995**, *6*, 1853; (d) Masui, M.; Shioiri, T. *Tetrahedron* **1995**, *51*, 8363; (e) Quallich, G. J.; Keavey, K. N.; Woodall, T. M. *Tetrahedron lett.* **1995**, *36*, 4729; (f) Shimizu, M.; Kamei, M.; Fujisawa, T. *ibid.* **1995**, *36*, 8607; (g) Reiners, I.; Wilken, J.; Martens, J. *Tetrahedron Asymmetry* **1995**, *6*, 3063; (h) Bach, J.; Berenguer, R.; Farras, J.; Garcia, J.; Meseguer, J.; Vilarrasa, J. *ibid.*, 2683; (i) Franot, C.; Stone, G. B.; Engeli, P.; Spöndlin, C.; Waldvogel, E. *ibid.* 2755; (j) Tillyer, R. D.; Boudreau, C.; Tschaen, D.; Dolling, U.-H.; Reider, P. J. *Tetrahedron Lett.* **1995**, *36*, 4337; (k) Otsuka, K.; Ito, K.; Katsuki, T. *SYNLETT* **1995**, 429; (l) Wallbaum, S.; Martens, J. *Tetrahedron Asymmetry* **1992**, *3*, 1475; (m) Deloux, L.; Srebnik, M. *Chem. Rev.* **1993**, *93*, 763; (n) Itsuno, S.; Sakurai, Y.; Ito, K.; Nakahama, S. *Bull. Chem. Soc. Jpn.*, **1987**, *60*, 395; (o) Corey, E. J.; Bakshi, R. K.; Shibata, S. *J. Am. Chem. Soc.* **1987**, *109*, 5551; (p) Corey, E. J.; Azimioara, M.; Sarshar, S. *Tetrahedron Letters* **1992**, *33*, 3429; (q) Mathre, D. J.; Thompson, A. S.; Douglas, A. W.; Hoogsteen, K.; Carroll, J. D.; Corley, E. G; Grabowski, E. J. J. *J. Org. Chem.* **1993**, *58*, 2880; (r) Douglas, A. W.; Tschaen, D. M.; Reamer, R. A.; Shi, Y.-J. *Tetrahedron Asymmetry* **1996**, *7*, 1303.

2. Nevalainen, V.; Uggla, R.; Sundberg, M. R. *Tetrahedron Asymmetry* **1995**, *6*, 1431.

3. Gaussian 94, Revision B.1, Frisch,M. J.; Trucks, G. W.; Schlegel, H. B.; Gill, P. M. W.; Johnson, B. G.; Robb, M. A.; Cheeseman, J. R.; Keith, T.; Petersson, G. A.; Montgomery, J. A.; Raghavachari, K.; Al-Laham, M. A.; Zakrzewski, V. G.; Ortiz, J. V.; Foresman, J. B.; Cioslowski, J.; Stefanov, B. B.; Nanayakkara, A.; Challacombe, M.; Peng, C. Y.; Ayala, P. Y.; Chen, W.; Wong, M. W.; Andres, J. L.; Replogle, E. S.; Gomperts, R.; Martin, R. L.; Fox, D. J.; Binkley, J. S.; Defrees, D. J.; Baker, J.; Stewart, J. P.; Head-Gordon, M.; Gonzalez, C.; Pople, J. A.; Gaussian, Inc., Pittsburgh PA, 1995.

4. Structure of the model **4a** (lone pairs of the *endo*-OH group *syn* to the carbonyl) optimized at the 3-21G level is shown below. The model **4b** was generated by rotating one B-O bond of the model shown below so that the torsion angles changed as follows: H-O-B-H (-140.3° -> -35.3°) and H-O-B-N (+105.4° -> -149.6°). Both of these models were found unstable as optimized further at the MP2/6-31G* level.

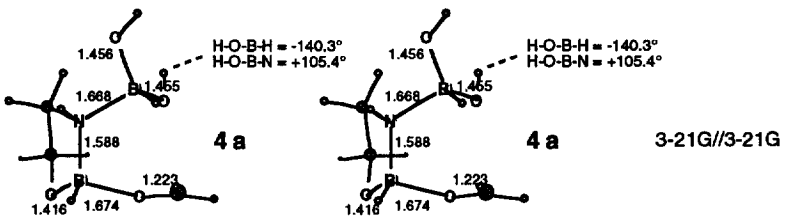

5. Nevalainen, V. *Tetrahedron Asymmetry* **1991**, *2*, 1133.

(*Received in UK* 28 *June* 1996)